BMJ Oncology

# Baseline tumour vessel perfusion as a non-invasive predictive biomarker for immune checkpoint therapy in non-small-cell lung cancer

Zhenhua Liu,[1,2,3] Ke Ma,[2] Qingzhu Jia,[4] Yunpeng Yang,[5] Peng Fan,[2] Ying Wang,[2] Junhui Wang,[2] Jiya Sun,[6] Liansai Sun,[2] Hongtai Shi,[7] Liang Sun,[8] Bo Zhu,[4] Wei Xu,[6] Li Zhang,[5] Rakesh K. Jain,[9] Songbing Qin,[1] Yuhui Huang [2,10]

**To cite:** Liu Z, Ma K, Jia Q, *et al*. Baseline tumour vessel perfusion as a non-invasive predictive biomarker for immune checkpoint therapy in non-small-cell lung cancer. *BMJ Oncology* 2024;**3**:e000473. doi:10.1136/bmjonc-2024-000473

► Additional supplemental material is published online only. To view, please visit the journal online (https://doi.org/10.1136/bmjonc-2024-000473).

ZL, KM, QJ and YY contributed equally.

Received 15 May 2024
Accepted 08 July 2024



For numbered affiliations see end of article.

**Correspondence to**
Dr Yuhui Huang; huangyh@suda.edu.cn and Dr Songbing Qin; qin92244@163.com

## ABSTRACT

**Objective** Current biomarkers for predicting immunotherapy response in non-small-cell lung cancer (NSCLC) are derived from invasive procedures with limited predictive accuracy. Thus, identifying a non-invasive predictive biomarker would improve patient stratification and precision immunotherapy.

**Methods and analysis** In this retrospective multicohort study, the discovery cohort included 205 NSCLC patients screened from ORIENT-11 and an external validation (EV) cohort included 99 real-world NSCLC patients. The 'onion-mode segmentation' method was developed to extract 'onion-mode perfusion' (OMP) from contrast-enhanced CT images. The predictive performance of OMP or its combination with the PD-L1 Tumour Proportion Score (TPS) was evaluated by the area under the curve (AUC).

**Results** High baseline OMP was associated with significantly longer survival and predicted patient response to combination anti-PD-(L)1 therapy in the discovery and EV cohorts. OMP complemented the PD-L1 TPS with superior predictive sensitivity (p=0.02). In the PD-L1 TPS<50% subgroup, OMP achieved an AUC of 0.77 for the estimation of treatment response (95% CI 0.66 to 0.86, p<0.0001). A simple bivariate model of OMP/PD-L1 robustly predicted therapeutic response in both the discovery (AUC 0.82, 95% CI 0.74 to 0.88, p<0.0001) and EV (AUC 0.80, 95% CI 0.67 to 0.89, p<0.0001) cohorts.

**Conclusion** OMP, derived from routine CT examination, could serve as a non-invasive and cost-effective biomarker to predict NSCLC patient response to immune checkpoint inhibitor-based therapy. OMP could be used alone or in combination with other biomarkers to improve precision immunotherapy.

### WHAT IS ALREADY KNOWN ON THIS TOPIC

Current biomarkers for immune checkpoint inhibitor (ICI) therapy are derived from invasive procedures with limited predictive accuracy, which is likely due to the heterogeneity of the tumour microenvironment. Preclinical studies show that increased tumour vessel perfusion by ICI therapy positively correlated with its efficacy, therefore, we proposed a novel approach to non-invasively predict patient responses to ICI therapy by extracting the global characteristics of baseline tumour vessel perfusion from contrast-enhanced CT (CECT) images.

## BACKGROUND

Immune checkpoint inhibitor (ICI) therapy based on blocking antibodies, including anti-programmed death 1 (anti-PD1), anti-programmed death ligand-1 (anti-PD-L1) and anti-cytotoxic T-lymphocyte antigen 4 (anti-CTLA4), has revolutionised cancer treatment; however, long-term survival benefits are achieved in less than 30% of patients with cancer.[1 2] Biomarkers, such as PD-L1 expression determined by the Tumour Proportion Score (TPS) and tumour mutation burden (TMB), have been approved by the US Food and Drug Administration for ICI therapy, but their predictive value is limited.[3–10] These biomarkers are derived from a biopsy or a portion of archived tumour tissues and thus may not fully reflect the spatiotemporal characteristics of the entire tumour due to the heterogeneity in the tumour microenvironment (TME). Moreover, these biomarkers require tumour biopsy, which may not be possible due to the poor performance status of patients or the location of tumours. Therefore, non-invasive biomarkers are urgently needed to improve patient selection for precision ICI therapy.

To reach cancer cells in a tumour, a blood-borne therapeutic agent must arrive in the tumour via its blood vessels. However, tumour vessels are structurally and functionally abnormal, which not only impairs the delivery of therapeutic agents, including immune cells but also creates an abnormal TME characterised by hypoxia and low pH that causes immunosuppression in tumours. In 2001, we hypothesised that agents that induce

### WHAT THIS STUDY ADDS

⇒ To our knowledge, this is the first study to use baseline tumour vessel perfusion as a predictive biomarker for patients with non-small-cell lung cancer (NSCLC). We extracted the global features of baseline tumour vessel perfusion from the patient's CECT images and named it 'onion-mode perfusion' (OMP). Higher values of OMP were associated with longer survival and predicted the response to ICI-based therapy in two independent patient cohorts with NSCLC. Conversely, baseline tumour size, also derived from CECT images, could only be served as a prognostic biomarker. In patients with programmed death ligand-1 (PD-L1)-low cancers, OMP was superior to PD-L1 in predicting therapeutic response. Moreover, a simple bivariate model of OMP and PD-L1 predicted the therapeutic response in the discovery and validation cohorts with the values of area under the curves above 0.80.

### HOW THIS STUDY MIGHT AFFECT RESEARCH, PRACTICE OR POLICY

⇒ CT is a non-invasive radiology scanning that is routinely used to measure tumour size in the clinic worldwide. Thus, OMP, a baseline global vessel perfusion feature extracted from CT images, could serve as a non-invasive and cost-effective predictive biomarker for ICI-based therapy. It can be easily integrated into current clinical practice procedures to substantially improve clinical decision-making of ICI-based therapy in NSCLC.

normalisation of the microenvironment can improve treatment outcomes.[11–14] Indeed, we demonstrated that judicious use of antiangiogenic agents—originally designed to starve tumours—could transiently normalise tumour vasculature, improve tumour perfusion, alleviate hypoxia, increase delivery of drugs and antitumour immune cells, and improve the outcome of various therapies, including immunotherapy.[13 15–19] Recent studies further showed that ICI therapy can increase tumour vessel perfusion and induce tumour vascular normalisation in a T cell-dependent manner.[18 19] Moreover, patients with cancer whose tumour perfusion increased with antiangionenic therapy had a better treatment outcome.[13] Similar to our clinical trials with antiangiogenic agents, increased vessel perfusion by ICI therapy strongly correlated with its efficacy in murine breast cancer models.[19] Moreover, in our neoadjuvant breast cancer trial, we found that the pretreatment microvascular density—an indirect measure of perfusion—correlated with the response to bevacizumab.[20] Based on these collective preclinical and clinical findings, we proposed a novel approach to predict individual tumour responses to ICI-based therapy by extracting the global characteristics of tumour vessel perfusion at baseline from contrast-enhanced CT (CECT) images.

We developed our approach using CECT images from a published randomised, double-blind, phase III study of non-squamous non-small-cell lung cancer (NSCLC) (ORIENT-11; ClinicalTrials.gov: NCT03607539). In this trial, all of the enrolled patients were histologically or cytologically confirmed to have stages IIIB–IV non-squamous NSCLC. Sintilimab (an anti-PD1 antibody from Innovent Biologics) combined with chemotherapy (pemetrexed and platinum) prolonged progression-free survival (PFS) and overall survival (OS) compared with chemotherapy alone.[21] By developing an 'onion-mode segmentation' method to extract the global features of tumour vessel perfusion from CECT images in a layer-by-layer manner, we first identified and then validated 'onion-mode perfusion' (OMP) in an independent cohort of patients as a potential non-invasive and cost-effective biomarker of an in situ tumour to predict patient response to ICI-based therapy in NSCLC.

## MATERIALS AND METHODS

### Study design and data sources

In this retrospective study, 'onion-mode segmentation' was conducted to extract OMP from CECT images in two independent cohorts of NSCLC patients who received anti-PD-(L)1 combination therapy.

The discovery cohort was derived from the ORIENT-11 study (ClinicalTrials.gov: NCT03607539), which included 397 patients with NSCLC from China who were treated between 23 August 2018 and 30 July 2019, and whose CECT images, treatment response and PD-L1 TPS data were available to us for analysis. We screened and obtained 205 patients with eligible CECT images for vessel perfusion analysis (129 patients received combination anti-PD1 therapy and 76 patients received chemotherapy alone) (online supplemental figure 1, methods and tables 1 and 2).

An independent external validation (EV) cohort was obtained from real-world patients with NSCLC (n=212) treated at Xinqiao Hospital (Chongqing, China) from 1 January 2018 to 31 December 2021. 99 patients with eligible CECT images were included in the analysis. Among them, 60 patients had PD-L1 TPS data (online supplemental figure 1, table 3 and methods). Patients' responses to therapy were assessed by Response Evaluation Criteria in Solid Tumour version 1.1 (RECIST V.1.1) (online supplemental methods).

Written informed consent was waived because all data were deidentified.

### OMP discovery in the discovery cohort

OMP data were extracted from the arterial phase of CECT images of patients with therapy. (a) Resampling the CECT images: Since the CECT images of the 205 patients came from 39 hospitals, all CECT images were resampled to 1×1×1 $mm^3$ using linear interpolation to reduce the difference in image quality due to different hospitals. (b) Outlining the volume of interest (VOI): 3D Slicer (V.4.11.0) software was used by a physician specialising in medical imaging and radiation therapy with 10 years of experience in delineating the tumour area to outline the area of the lung tumour. The threshold of tumour outlines was set from −50 to 200 Hounsfield units to semiautomatically sketch tumour areas. (c) Onion-mode segmentation: The 3D Slicer software was set to simulate

the 'onion-peeling' method to segment the VOI. The VOI was globally divided layer by layer from the outermost to the innermost with a thickness of 1 mm per layer (ie, one-pixel thickness). (d) OMP calculation: Based on Python (V.3.7.4), the Simple ITK package (V.1.2.4) was used to extract the data of VOI layers. The original value of each layer was subjected to max-min normalisation by Value_normalised=(value_origin−value_min)/(Value_max−value_min). The value of layers 2, 3, …, n based on the respective layer 1 as the baseline of each VOI was taken as the OMP. (e) Replicate analysis: 30 CECT images were randomly selected from the 205 images. Another physician with 10 years of experience in medical imaging and radiation therapy conducted procedures b, c and d to calculate the OMP independently. Intergroup and intragroup correlation analyses were used to evaluate the repeatability of the VOI. Original values were provided in online supplemental file 2.

### Model building

In the discovery cohort, the cases from the first six hospitals were served as the validation set, and the remaining cases from the other 33 hospitals were served as the training set (online supplemental table 4). The cutoff value of OMP was determined by the receiver operator characteristic (ROC) curve. The effectiveness of the model diagnosis with OMP, TPS or their combination was assessed by area under the curves (AUCs) using the DeLong test.[22] For detailed information, please refer to online supplemental methods. Original values were provided in online supplemental file 2.

### OMP validation

99 eligible real-world patients with NSCLC screened from 212 patients treated at Xinqiao Hospital (Chongqing, China) with combination anti-PD-(L)1 therapy formed an independent EV cohort (online supplemental figure 1 and table 3). The procedures of CECT image resampling, VOI outlining, onion-mode segmentation and OMP analysis were conducted in the EV cohort as described above in the discovery cohort. The association of OMP with PFS and the predictive performance of OMP alone or in combination with PD-L1 TPS were analysed by the Kaplan-Meier method and AUCs, respectively. Original values were provided in online supplemental file 2.

### Statistical analysis

Statistical analyses were conducted with Prism software (V.8, GraphPad) and MedCalc (V.20.019). Data are presented as the mean±SEM. Data were first confirmed for their normal distribution using the Kolmogorov-Smirnov test. The balance of baseline clinical characteristics in different patient cohorts was evaluated by Fisher's exact test or $\chi^2$ test. Unpaired two-tailed Student's t-tests were used to compare the differences between the two groups. PFS or OS was estimated by the Kaplan-Meier method. Hazard Ratios (HRs) and the 95% confidence intervals (CIs) were computed using the Cox proportional hazard model, and the survival differences between groups were determined by the log-rank test. The difference in predictive sensitivity between OMP and PD-L1 TPS ≥50% was analysed by McNemar's test. ROC curves and AUCs were used to evaluate the prediction models. The association between variables and the integration of multiple biomarkers to predict responders was developed by multivariable logistic regression analysis. DeLong's test was used to calculate the 95% CI and the p value of the AUCs. All statistical tests were two sided, and the results were considered statistically significant at $p<0.05$.

## RESULTS

### OMP development

The distribution and intensity of tumour vessel perfusion within the TME are spatially heterogeneous,[12 23 24] thus simply assessing overall tumour vessel perfusion may not accurately reflect the critical characteristics of vessel perfusion of a given tumour. Given that tumour vessel perfusion is relatively high in the tumour periphery but relatively low toward the tumour centre and that contrast agent enters the tumour parenchyma via perfused blood vessels and predominantly distributes around the area with function vessels (figure 1A),[19 23 25–27] we explored what we termed OMP to characterise the characteristics of baseline tumour vessel perfusion (figure 1B). Briefly, we designed an 'onion-mode segmentation' approach to extract the value of baseline tumour vessel perfusion globally in a layer-by-layer manner from the CECT images of the 205 patients with NSCLC (figure 1B). The thickness of each layer was 1 mm from the outermost (the baseline layer) to the innermost (the last layer). To exclude the potential influences of different CT scans and the different basic characteristics of tumours on the values representing tumour vessel perfusion, we normalised the value of each layer to the baseline layer in a given tumour to obtain their relative OMP values.

### OMP and clinical parameters

The discovery cohort included 129 patients with anti-PD1 combination therapy and 76 patients with chemotherapy alone, who were screened from the ORIENT-11 study composed of 397 patients with NSCLC.[21] The baseline clinical characteristics between the included patient cohorts and the original patient cohorts were comparable, suggesting that the screening did not cause bias (online supplemental table 1).

The two independent cohorts included 304 patients with non-squamous or squamous NSCLC and had overall balanced clinical characteristics (online supplemental tables 2 and 3). The discovery and EV cohorts had overall comparable proportions of patients with PD-L1 TPS≥50% (50 of 129 (39%) vs 18 of 60 (30%)), male sex (98 of 129 (76%) vs 89 of 99 (90%)), age older than 60 (66 of 129 (51%) vs 54 of 99 (55%)), responders (77 of 129 (60%) vs 54 of 99 (55%)) and OMP≥0.32 (71 of 129 (55%) vs 40 of 99 (40%)).

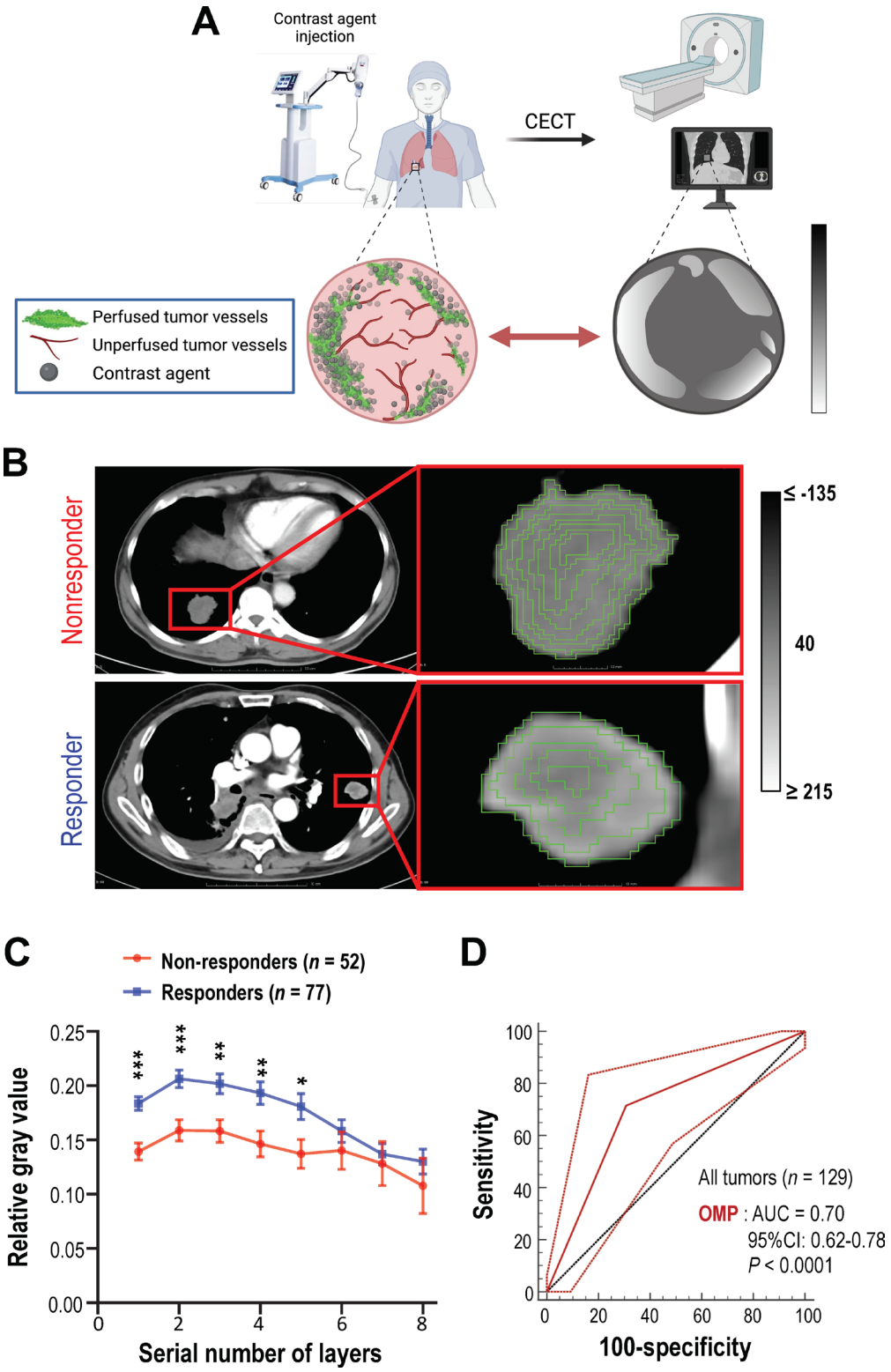


**Figure 1** OMP development and the predictive performance of OMP in patients with non-small cell lung cancer (NSCLC). The contrast-enhanced CT (CECT) images of NSCLC patients prior to the combination of sintilimab (anti-PD1) and chemotherapy (pemetrexed and platinum) (n=129) were analysed by using 'onion-mode segmentation' to obtain 'onion-mode perfusion' (OMP) of tumour tissues. (A) Schematic diagram shows the relationship between vessel perfusion and the distribution of contrast agent in CECT images. After intravenous injection, contrast agent enters the tumour parenchyma via perfused tumour blood vessels and predominantly distributes around the area with functional vessels. (B) Representative CECT images with 'onion-mode segmentation'. (C) The values of OMP in responsive versus non-responsive NSCLC patients. Data are presented as the mean±SEM. *p<0.05, **p<0.01, ***p<0.001 (two-tailed Student's t-tests). (D) The ROC curve of OMP to predict the response to anti-PD1 combination therapy in NSCLC patients. The cut-off value of baseline OMP was 0.32. The AUC was analysed by DeLong's test. AUC, area under the curve; ROC, receiver operator characteristic.

In addition, the results from the Cox proportional hazards regression model showed that OMP, PD-L1 TPS and the value of ECOG (Eastern Cooperative Oncology Group) were effective factors influencing patient prognosis while the other clinical characteristics, such as histology, smoking history, baseline TMB, brain metastases, liver metastasis, stage, sex and age, did not influence patient prognosis (online supplemental table 5). Thus, OMP is a prognostic factor for patients with NSCLC.

### High baseline OMP predicts response to anti-PD1 combination therapy

In the anti-PD1 combination treatment arm in the discovery cohort, the OMP values of each of the layers 1–5 in the responders were significantly higher than those in the corresponding layers in the non-responders (figure 1C). To determine the relationship between baseline OMP and the efficacy of anti-PD1 combination therapy, we quantified $OMP_{1-2}$, $OMP_{1-3}$, or $OMP_{1-4}$ of each tumour tissue by adding the sum of the relative values of the first 2, 3 or four layers, respectively. The cut-off values of $OMP_{1-2}$, $OMP_{1-3}$ or $OMP_{1-4}$ were calculated based on the ROC curves as described previously.[22] Significantly longer OS was associated with higher baseline levels of OMP (online supplemental figure 2), where $OMP_{1-2}$ showed the best association with longer OS. Thus, we used $OMP_{1-2}$ and its cut-off value of 0.32 for the remainder of our OMP-based assessments. For the predictive performance of OMP, the AUC for the prediction of the patient's response to anti-PD1 combination therapy by baseline OMP was 0.70 (p<0.001) (figure 1D), whereas the AUC of OMP in patients with NSCLC with chemotherapy alone was 0.54 (p=0.49) (online supplemental figure 3).

### Baseline tumour size is a prognosis factor but fails to predict patient response to ICI-based therapy

Since small tumours generally have higher vessel perfusion than large tumours, this raised the question of whether the predictive value of OMP is simply due to tumour size. Previous reports also suggest that baseline tumour size (BTS) is a prognostic factor for patients receiving ICI therapy.[28 29] Thus, we quantified BTS following a previously described protocol[28] and quantified BTS by adding the sum of the longest dimensions of all detected lesions in NSCLC patients derived from a Phase III study (ClinicalTrials.gov: NCT03607539). Patients were assigned as small or large BTS subgroups based on the median of the BTS value. In the discovery cohort (n=205), OMP was inversely correlated with BTS, and BTS in OMP-low subgroup was significantly larger than that of OMP-high subgroup (online supplemental figure 4). In the whole cohort (n=397), the small BTS subgroup had significantly longer PFS and OS compared with the large BTS subgroup in the anti-PD1 combination treatment arm (n=266), whereas no such distinction in survival benefits was detected for the chemotherapy alone arm (n=131) (figure 2). We then evaluated the predictive performance of BTS by calculating the area under the ROC curves as described previously[22]; unfortunately, the AUC of BTS was 0.52 (p=0.68) (online supplemental figure 5), suggesting that BTS per se cannot predict patient response to anti-PD1 combination therapy in NSCLC.

### OMP complements PD-L1 TPS with superior predictive sensitivity

Because baseline PD-L1 TPS is an approved predictive biomarker,[3 9] we then compared the performance of OMP and PD-L1 TPS in predicting the response of patients with NSCLC to anti-PD1 combination treatment. The AUC of PD-L1 TPS ≥50% was 0.71 (p<0.0001), whereas the AUC of PD-L1 TPS in patients with NSCLC with chemotherapy alone was 0.57 (p=0.25) (online supplemental figure 6). Although the AUC values of PD-L1 TPS and OMP were comparable, the predictive sensitivity of OMP tended to be higher than that of PD-L1 TPS ≥50% (71.43% vs 55.84%, McNemar's test p=0.09, n=129) (online supplemental figure 7). In addition, multivariate logistic regression analysis showed that OMP and PD-L1 TPS can independently predict patient response to anti-PD1 combination therapy in NSCLC (p<0.001). By contrast, brain metastasis, liver metastasis, ECOG, smoking, stage, baseline tumour burden, pathology, sex and age could not be independently predicted (online supplemental table 6). Taken together, the data show that baseline OMP is superior to PD-L1 TPS in predicting patient response to anti-PD1 combination therapy in NSCLC.

Given our results indicating that both the OMP and PD-L1 TPS can predict the response to anti-PD1 combination therapy and considering that patients exhibit wide variation in baseline values of the OMP and PD-L1 TPS, we next explored which biomarker performs better for specific patient subgroups. In the PD-L1 TPS<50% subgroup, high baseline OMP was associated with significantly longer OS (19.6 vs 9.6 months, HR 0.39, 95% CI 0.22 to 0.68, p=0.0009), and the AUC by OMP for predicting therapeutic response was 0.77 (p<0.0001) (figure 3A). In the OMP low (<0.32) subgroup, PD-L1 TPS≥50% was predictive of longer OS in patients with NSCLC who received anti-PD1 combination therapy (NR vs 9.6 months, HR 0.29, 95% CI 0.13 to 0.65, p=0.0023), with an AUC of 0.81 (p<0.0001) (figure 3B). Together, these results suggest that the predictive performance of OMP and PD-L1 TPS is complementary. OMP outperforms PD-L1 TPS for predicting the response to anti-PD1 combination therapy in NSCLC patients with PD-L1 TPS<50%.

### A bivariate model of OMP and PD-L1 TPS robustly predicts response to anti-PD1 combination therapy

Seeking to extend the utility of these biomarkers to the whole cohort, ideally combining the relative merits of OMP and PD-L1 TPS, we analysed the predictive performance of OMP plus PD-L1 TPS and the AUC reached 0.82 (p<0.0001) (figure 4A). We further performed five-fold cross-validation on this model. The AUCs by OMP

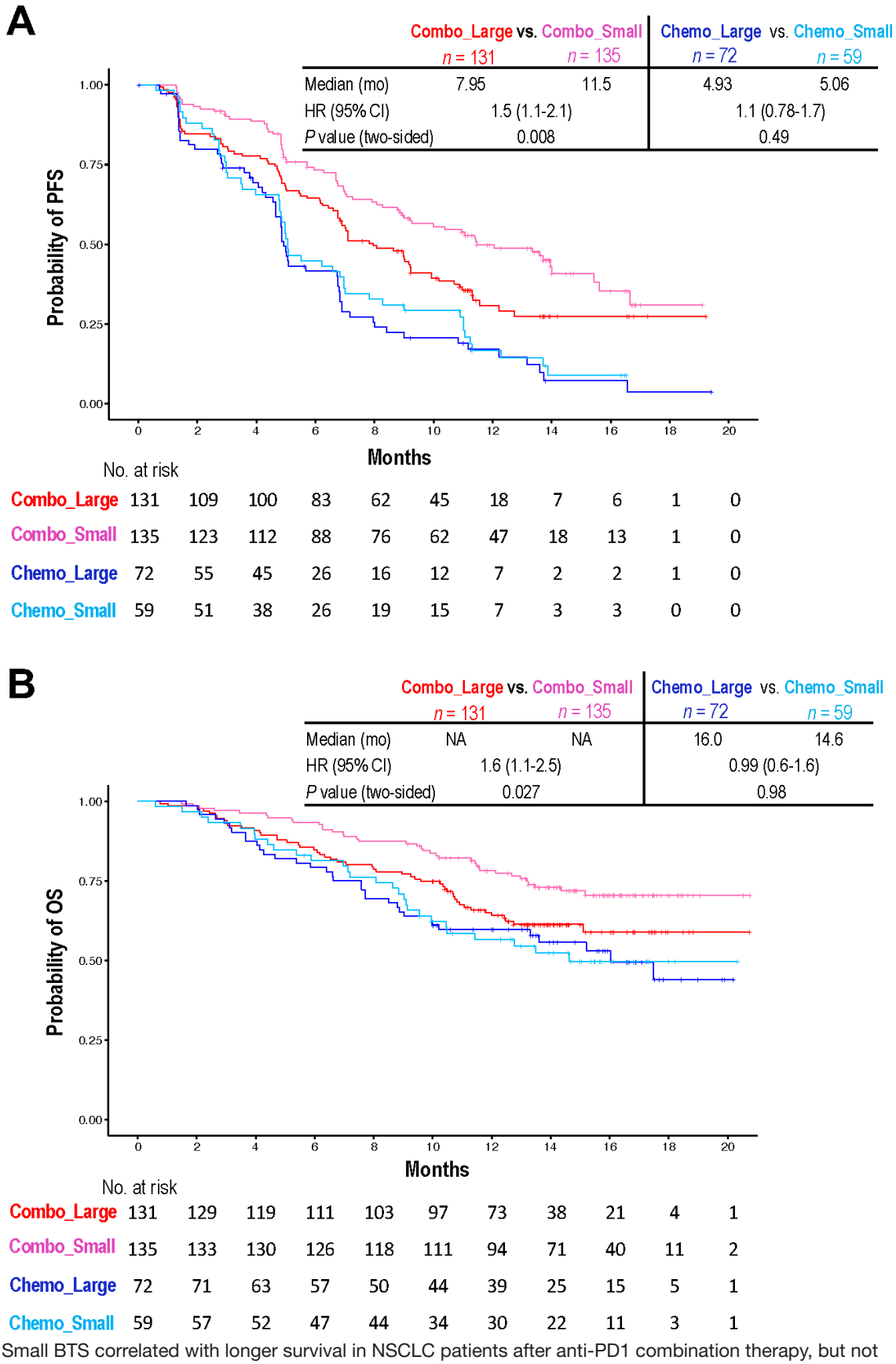


**Figure 2** Small BTS correlated with longer survival in NSCLC patients after anti-PD1 combination therapy, but not chemotherapy. Kaplan-Meier estimate of PFS (A) and OS (B) in patients with NSCLC. P values were determined by log-rank tests. Combo-large and combo-small: the combination of sintilimab (anti-PD1) and chemotherapy (pemetrexed and platinum) with large or small BTS. BTS, baseline tumour size; NSCLC, non-small-cell lung cancer; OS, overall survival; PFS, progression-free survival.

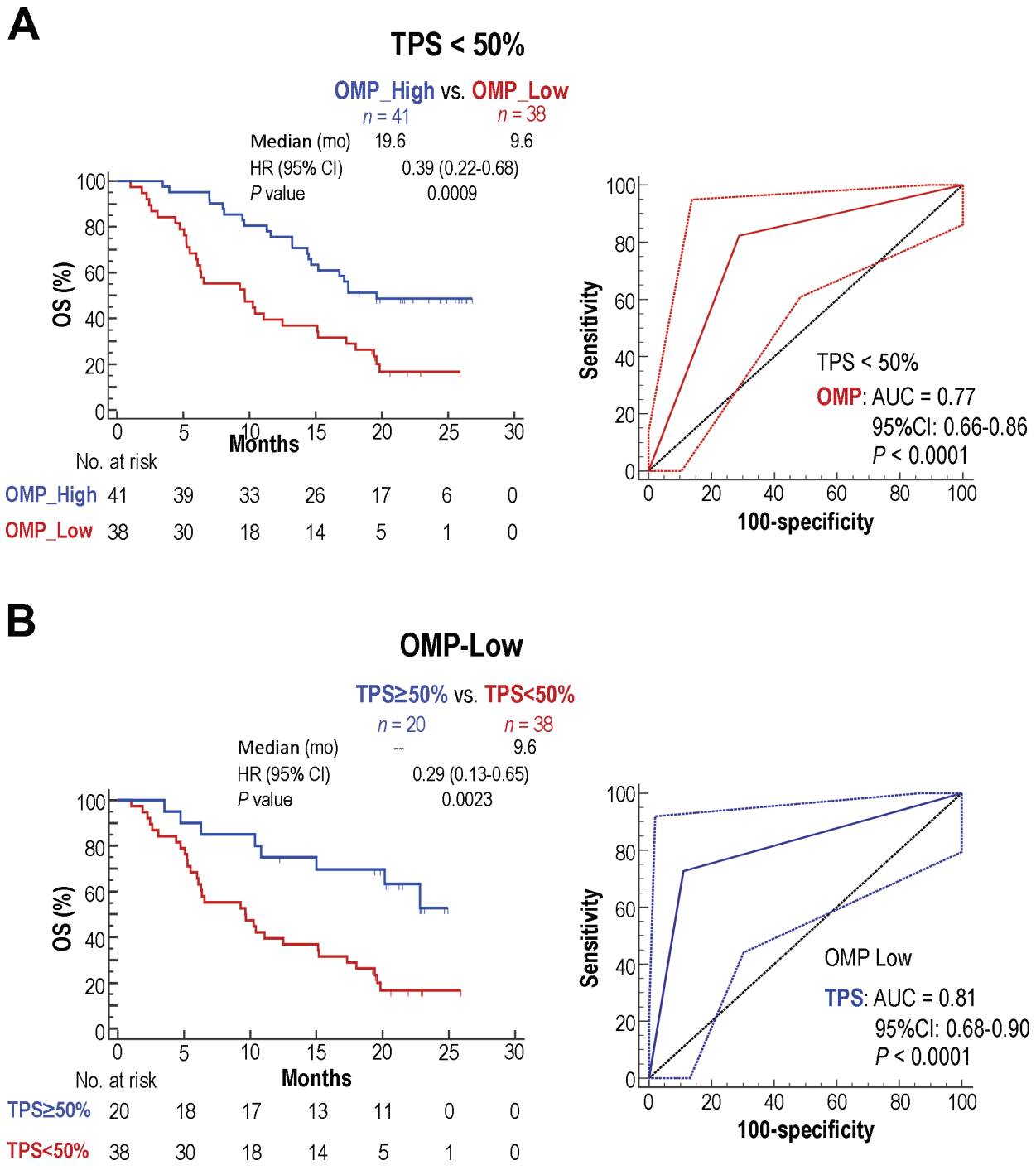


**Figure 3** The complementary predictive performance of OMP and PD-L1 TPS in the subgroup of patients with NSCLC. (A) In the PD-L1 TPS<50% subgroup of patients with NSCLC, Kaplan-Meier analysis of OS after anti-PD1 combination therapy stratified by baseline OMP-high or OMP-low (left), and the ROC curve of OMP to predict therapeutic response (right). (B) In the OMP-low subgroup of patients with NSCLC, Kaplan-Meier analysis of OS after anti-PD1 combination therapy stratified by baseline PD-L1 TPS≥50% or <50% (left) and the ROC curve of PD-L1 TPS to predict therapeutic response (right). The cut-off value of baseline OMP was 0.32. The difference between survival curves was determined by log-rank tests, and the AUCs were analysed by DeLong's tests. AUC, area under the curve; OMP, onion-mode perfusion; OS, overall survival; ROC, receiver operator characteristic; TPS, Tumour Proportion Score.

and PD-L1 TPS were 0.92, 0.86, 0.85, 0.73 and 0.79, and their average was 0.83 (figure 4B). The results show that the bivariate model is robust and stable. To evaluate the potential of OMP and PD-L1 TPS to select sensitive patients for ICI-based therapy, we also divided the 129 patients with NSCLC into a validation set (40 patients from the first 6 hospitals) and a training set (89 patients from all the other hospitals) (online supplemental figure 1 and table 4). The AUC for the prediction of tumour response to anti-PD1 combination therapy by OMP and

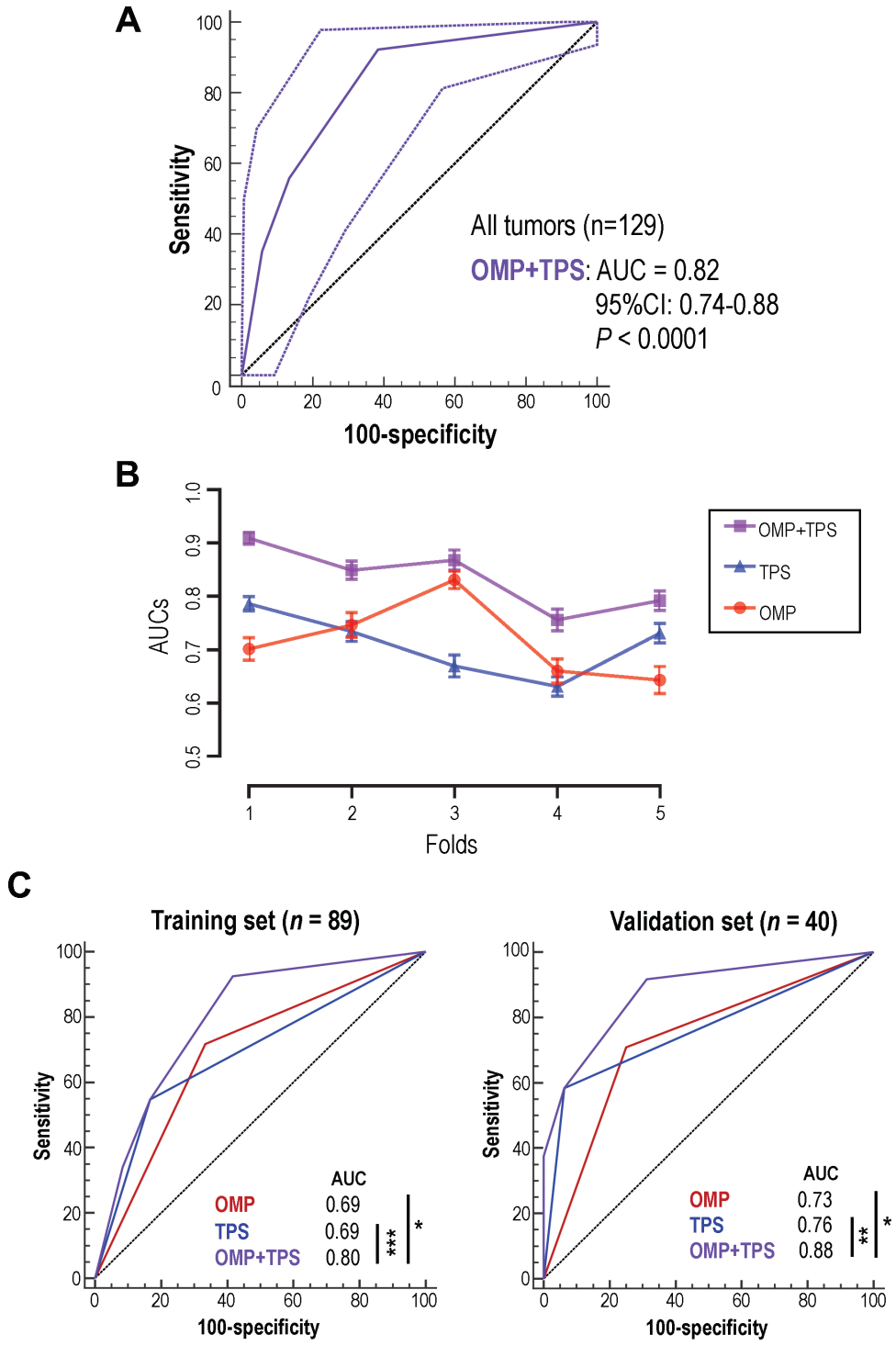


**Figure 4** The predictive performance of OMP, PD-L1 TPS or both in patients with NSCLC. (A) ROC curve to predict the response to anti-PD1 combination therapy. (B) Fivefold cross-validation of the bivariate model. (C) The 129 patients with NSCLC were divided into training and validation sets with balanced clinical characteristics. ROC curves to predict the response to anti-PD1 combination therapy in the training set (left) and validation set (right) of patients with NSCLC. The cut-off values of baseline OMP and PD-L1 TPS were 0.32 and 50%, respectively. *p<0.05, **p<0.01, ***p<0.001. The AUCs were analysed by DeLong's tests. AUC, area under the curve; NSCLC, non-small-cell lung cancer; OMP, onion-mode perfusion; ROC, receiver operator characteristic; TPS, Tumour Proportion Score.

PD-L1 TPS in the training set was 0.80 and that in the validation set was 0.88 (figure 4C). Together, these results show robust predictive performance of the bivariate model of baseline OMP and PD-L1 TPS.

To evaluate the potential of the bivariate model of baseline OMP and PD-L1 TPS to predict response to ICI-based therapy in real-world patients, we screened an independent EV cohort including 212 patients with NSCLC

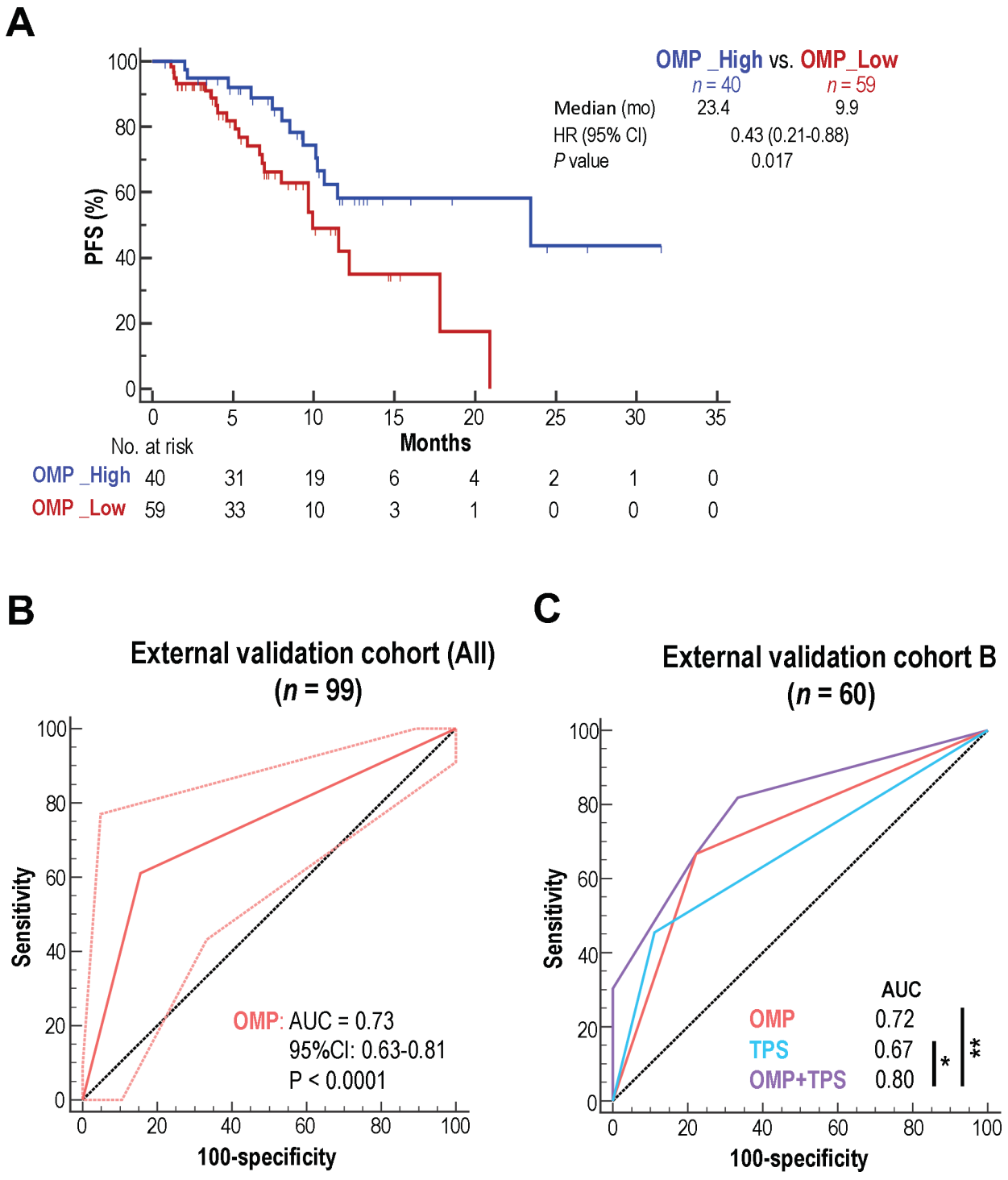


**Figure 5** The predictive performance of the OMP/PD-L1 TPS pair in real-world patients with NSCLC. (A) Kaplan-Meier analysis of PFS after anti-PD-(L)1 combination therapy stratified by baseline OMP-high or OMP-low. (B) The ROC curve of OMP to predict therapeutic response. (C) ROC curves to predict therapeutic response. The cut-off values of baseline OMP and PD-L1 TPS were 0.32 and 50%, respectively. *p<0.05, **p<0.01. The difference between survival curves was determined by log-rank tests, and the AUCs were analysed by DeLong's tests. AUC, area under the curve; NSCLC, non-small-cell lung cancer; OMP, onion-mode perfusion; PFS, progression-free survival; ROC, receiver operator characteristic; TPS, Tumour Proportion Score.

treated with anti-PD-(L)1 combination therapy in Xinqiao Hospital (Chongqing, China) and obtained 99 patients with eligible CECT images (online supplemental figure 1 and table 3). Remarkably, high baseline OMP was associated with significantly longer PFS (23.4 vs 9.9 months, HR 0.43, 95% CI 0.21 to 0.88, p=0.017) than low OMP in the 99 real-world patients with NSCLC (figure 5A). The AUC for the prediction of tumour response to the combination therapy by OMP was 0.73 (p<0.0001, n=99) (figure 5B). In the 60 real-world patients with NSCLC

with both CECT images and PD-L1 TPS data, high baseline OMP was still associated with significantly longer PFS (23.4 vs 9.7 months, HR 0.30, 95% CI 0.12 to 0.76, p=0.012) than low OMP, while PD-L1 TPS≥50% was not associated with longer PFS (23.4 vs 10.1 months, HR 0.56, 95% CI 0.23 to 1.34, p=0.19) than PD-L1 TPS<50% (online supplemental figure 8). The AUC of the OMP plus PD-L1 TPS for predicting the therapeutic response was 0.80 (p<0.0001), the AUC of the OMP was 0.72, and the AUC of the PD-L1 TPS was 0.67 (figure 5C). Moreover, the predictive sensitivity of OMP was significantly higher than that of PD-L1 TPS≥50% when combining the 60 patients with 129 patients from the discovery cohort (McNemar's test p=0.02, n=189). Collectively, the data show that a bivariate model of baseline OMP and PD-L1 TPS exhibits robust predictive performance in patients with NSCLC.

## DISCUSSION

Low response rates to ICI-based therapy have motivated enormous efforts to identify and employ reliable biomarkers to stratify sensitive patients.[5 9 30] Currently, available biomarkers are generally derived from invasive procedures and the analysis of a small region of tumour tissue. Here, we developed 'onion-mode segmentation' to analyse CECT images of entire tumours and discovered OMP as a novel tumour vessel perfusion-based predictive biomarker for ICI-based therapy. OMP can predict the response to anti-PD1 combination therapy in patients with NSCLC. Moreover, OMP complemented the PD-L1 TPS with superior predictive sensitivity. Notably, a simple bivariate model of OMP and PD-L1 TPS robustly predicted the response of patients with NSCLC to anti-PD1 combination therapy with AUCs higher than 0.80. As CECT is a non-invasive form of radiology scanning that is routinely used to measure tumour sizes in the clinic worldwide, OMP appears to be a cost-effective and reliable predictive biomarker that can be used on its own or easily integrated with other biomarkers to improve clinical decision-making for ICI-based therapy.

Tumours are heterogeneous and change dynamically during their progression and in response to various treatments. Therefore, an ideal biomarker should be able to reflect the spatiotemporal properties of an in situ TME. Baseline OMP can be extracted from CECT images to evaluate the extent of tumour vessel perfusion globally and in real time. OMP can reflect tumour tissue oxygenation. Good perfusion (ie, high OMP) leads to reduced tumour tissue hypoxia, which in turn contributes to the formation of an immunosupportive TME to facilitate antitumour immunity.[14 31] Elevated tumour vessel perfusion on immunological interventions has been shown to be associated with higher intratumoural $CD8^+$ T cells,[19 23] suggesting that OMP might be able to reflect the quantity and status of intratumoural $CD8^+$ T cells. Collectively, the levels of OMP could mirror the characteristics of the entire tumour immune microenvironment. This could be a reason that OMP can predict a patient's response to ICI-based therapy. In addition, hypoxia-induced factor 1α can bind to the *PD-L1* promotor and induce its expression,[32] though *PD-L1* can be upregulated by IFNγ and some oncogenic signalling.[33] In OMP-low tumours with high PD-L1 expression, PD1/PD-L1 blockade therapy may activate intratumoural T cells, which in turn may improve tumour vessel perfusion.[18 19] The initiation of immune-vascular crosstalk may lead to the suppression of tumour growth.[19 34] This is one possible reason that PD-L1 TPS≥50% can predict the immunotherapy response in OMP-low tumours.

Although smaller sizes of tumours usually have higher OMP and respond better to immunotherapy, baseline tumour volume cannot predict patient response to chemotherapy or anti-PD1 combination therapy. The key question is how small of a tumour should be considered as a small tumour. There are no reliable criteria for determining the threshold of tumour size. Moreover, the relationship between tumour size and tumour perfusion is not linear. In some preclinical studies, tumour perfusion has been shown to decrease exponentially with tumour size.[27] Hence, baseline tumour size alone may not be a robust predictive biomarker.

Several previous reports have used CT images to extract radiomic features to manifest the properties of tumours or the TME.[35 36] For example, the linkage between the radiomic signature and *CD8* gene transcription helped to predict the immune phenotype of a tumour.[35] RNA sequencing generally uses biopsy or a portion of archived samples, which may still confront tumour heterogeneity and the disconnection between gene transcription and immune cell function. CT-derived quantitative vessel tortuosity is a feature of tumour vessel morphology, which could reflect some immunological properties of the TME.[36] However, tumour vessel perfusion is the most critical parameter of the tumour vasculature and can reflect the global status of tumour-infiltrating T cells.[12 18 19 23 24 34] Thus, OMP was developed according to the pathophysiological nature of tumour blood vessels and the tumour immune microenvironment and could be a more reliable and practical imaging biomarker for ICI-based therapy.

The current study also had limitations. This is a retrospective analysis, although some data were from a prospective clinical study. Therefore, the number of patients eligible for OMP analysis was relatively small, and we could not analyse the relationship between OMP and intratumoural T-cell function. Thus, these findings may need to be validated by prospective studies. Moreover, different types of solid tumours are often examined by different radiology approaches, for example, CT for lung cancer, MRI for brain cancer and ultrasound for liver cancer. The translation of OMP from CECT to other radiological images may need further investigation.

## CONCLUSIONS

These findings in the two cohorts suggest that higher baseline levels of OMP, a global feature of tumour vessel perfusion, are associated with a longer survival benefit and can predict the response of patients with NSCLC to ICI-based therapy. Moreover, OMP complements the PD-L1 TPS with superior predictive sensitivity. A simple bivariate model of baseline OMP and PD-L1 TPS exhibits robust predictive performance in patients with NSCLC. Thus, OMP could serve as a non-invasive, cost-effective and TME-based biomarker to improve precision immunotherapy. Large-scale prospective studies are warranted to validate these results.

**Author affiliations**
[1]Department of Radiotherapy, State Key Laboratory of Radiation Medicine and Prevention, First Affiliated Hospital of Soochow University, Suzhou, Jiangsu, China
[2]Cyrus Tang Medical Institute, State Key Laboratory of Radiation Medicine and Prevention, Collaborative Innovation Center of Hematology, Soochow University, Suzhou, Jiangsu, China
[3]Department of Radiotherapy, Yancheng First Hospital Affiliated Hospital of Nanjing University Medical School, Yancheng, Jiangsu, China
[4]Institute of Cancer, Third Military Medical University, Chongqing, Chongqing, China
[5]State Key Laboratory of Oncology in South China, Guangdong Provincial Clinical Research Center for Cancer, Sun Yat-sen University Cancer Center, Guangzhou, Guangdong, China
[6]New Drug Biology and Translational Medicine, Innovent Biologics Inc, Suzhou, Jiangsu, China
[7]Department of Radiation Oncology, Yancheng Third People's Hospital, Yancheng, Jiangsu, China
[8]State Key Laboratory of Radiation Medicine and Protection, School of Radiation Medicine and Protection, Soochow University, Suzhou, Jiangsu, China
[9]Department of Radiation Oncology, Massachusetts General Hospital, Harvard Medical School, Boston, Massachusetts, USA
[10]Institute of Pediatric Research, Children's Hospital of Soochow University, Suzhou, Jiangsu, China

**Acknowledgements** The authors would like to thank Drs Yueping Shen, Dan Duda, Hang Lee and Sonu Subudhi for their helpful input on our manuscript.

**Contributors** YH conceived and directed the study. ZL and YH developed the methods and analysed the clinic-related data. QJ, YY, LZ, BZ and WX provided CT images, collected patient information or conducted data analysis. KM, PF, YW, JW, JS, LiansaiS, HS and LiangS collected patient information and conducted data analysis. ZL, KM, QJ, YY, BZ, WX, LZ, RKJ, SQ and YH interpreted the results. RKJ, SQ and YH wrote the manuscript with input from all the other authors. YH acts as the guarantor of this study.

**Funding** This work was supported by grants from the National Natural Science Foundation of China (82150106 to YH, 82073337 to SQ, 81972877 to YH, 82272789 to LZ and 82241232 to LZ), Jiangsu Provincial Medical Key Discipline (ZDXK202235 to SQ), Interdisciplinary Basic Frontier Innovation Program of Suzhou Medical College of Soochow University(YXY2303028 to YH), the 2022 Jiangsu Science and Technology Plan Special Fund (Key R&D Plan Social Development) (BE2022727 to SQ), the Ludwig Cancer Center at Harvard (RKJ), Nile Albright Research Foundation (RKJ), Jane's Trust Foundation (RKJ), the National Foundation for Cancer Research(RKJ), the Collaborative Innovation Center of Hematology and the Priority Academic Program Development of Jiangsu Higher Education Institutions.

**Competing interests** RKJ received consultant fees from Cur, DynamiCure, Elpis, Innocoll, Merck, SPARC and SynDevRx; owns equity in Accurius, Enlight and SynDevRx; serves on the Boards of Trustees of Tekla Healthcare Investors, Tekla Life Sciences Investors, Tekla Healthcare Opportunities Fund and Tekla World Healthcare Fund and received grants from Boehringer Ingelheim and Sanofi. Neither any reagent nor any funding from these organisations was used in this study. JS is an employee of Innovent Biologics. WX used to be an employee of Innovent Biologics. All the other authors declare no competing interests.

**Patient and public involvement** Patients and/or the public were not involved in the design, or conduct, or reporting, or dissemination plans of this research.

**Patient consent for publication** Not applicable.

**Provenance and peer review** Not commissioned; externally peer reviewed.

**Data availability statement** Data are available on reasonable request. All data relevant to the study are included in the article or uploaded as online supplemental information.



**ORCID iD**
Yuhui Huang http://orcid.org/0000-0003-1985-3575

## REFERENCES

1 Topalian SL, Drake CG, Pardoll DM. Immune checkpoint blockade: a common denominator approach to cancer therapy. *Cancer Cell* 2015;27:450–61.
2 Sharma P, Goswami S, Raychaudhuri D, *et al*. Immune checkpoint therapy-current perspectives and future directions. *Cell* 2023;186:1652–69.
3 Garon EB, Rizvi NA, Hui R, *et al*. Pembrolizumab for the treatment of non-small-cell lung cancer. *N Engl J Med* 2015;372:2018–28.
4 Le DT, Uram JN, Wang H, *et al*. PD-1 blockade in tumors with mismatch-repair deficiency. *N Engl J Med* 2015;372:2509–20.
5 Havel JJ, Chowell D, Chan TA. The evolving landscape of biomarkers for checkpoint inhibitor immunotherapy. *Nat Rev Cancer* 2019;19:133–50.
6 André T, Shiu K-K, Kim TW, *et al*. Pembrolizumab in microsatellite-instability-high advanced colorectal cancer. *N Engl J Med* 2020;383:2207–18.
7 Marabelle A, Fakih M, Lopez J, *et al*. Association of tumour mutational burden with outcomes in patients with advanced solid tumours treated with pembrolizumab: prospective biomarker analysis of the multicohort, open-label, phase 2 KEYNOTE-158 study. *Lancet Oncol* 2020;21:1353–65.
8 Forde PM, Chaft JE, Smith KN, *et al*. Neoadjuvant PD-1 blockade in resectable lung cancer. *N Engl J Med* 2018;378:1976–86.
9 Doroshow DB, Bhalla S, Beasley MB, *et al*. PD-L1 as a biomarker of response to immune-checkpoint inhibitors. *Nat Rev Clin Oncol* 2021;18:345–62.
10 Obeng RC, Nasti TH, Martens K, *et al*. Characterisation of clinical response and transcriptional profiling of proliferating CD8 T cells in the blood of cancer patients after PD-1 monotherapy or combination therapy. *BMJ Oncology* 2024;3:e000328.
11 Jain RK. Normalizing tumor vasculature with anti-angiogenic therapy: a new paradigm for combination therapy. *Nat Med* 2001;7:987–9.
12 Jain RK. Normalization of tumor vasculature: an emerging concept in antiangiogenic therapy. *Science* 2005;307:58–62.
13 Jain RK. Normalizing tumor microenvironment to treat cancer: bench to bedside to biomarkers. *J Clin Oncol* 2013;31:2205–18.
14 Jain RK. Antiangiogenesis strategies revisited: from starving tumors to alleviating hypoxia. *Cancer Cell* 2014;26:605–22.
15 Huang Y, Yuan J, Righi E, *et al*. Vascular normalizing doses of antiangiogenic treatment reprogram the immunosuppressive tumor microenvironment and enhance immunotherapy. *Proc Natl Acad Sci U S A* 2012;109:17561–6.
16 Martin JD, Seano G, Jain RK. Normalizing function of tumor vessels: progress, opportunities, and challenges. *Annu Rev Physiol* 2019;81:505–34.

17 Shigeta K, Datta M, Hato T, *et al*. Dual programmed death receptor-1 and vascular endothelial growth factor receptor-2 blockade promotes vascular normalization and enhances antitumor immune responses in hepatocellular carcinoma. *Hepatology* 2020;71:1247–61.
18 Tian L, Goldstein A, Wang H, *et al*. Mutual regulation of tumour vessel normalization and immunostimulatory reprogramming. *Nature* 2017;544:250–4.
19 Zheng X, Fang Z, Liu X, *et al*. Increased vessel perfusion predicts the efficacy of immune checkpoint blockade. *J Clin Invest* 2018;128:2104–15.
20 Tolaney SM, Boucher Y, Duda DG, *et al*. Role of vascular density and normalization in response to neoadjuvant bevacizumab and chemotherapy in breast cancer patients. *Proc Natl Acad Sci U S A* 2015;112:14325–30.
21 Yang Y, Zhou H, Zhang L, *et al*. Response to letter to the editor: efficacy and safety of sintilimab plus pemetrexed and platinum as first-line treatment for locally advanced or metastatic nonsquamous NSCLC: a randomized, double-blind, phase 3 study (ORIENT-11). *J Thorac Oncol* 2020;15:e191–2.
22 DeLong ER, DeLong DM, Clarke-Pearson DL. Comparing the areas under two or more correlated receiver operating characteristic curves: a nonparametric approach. *Biometrics* 1988;44:837–45.
23 Zhang N, Yin R, Zhou P, *et al*. DLL1 orchestrates $CD8^+$ T cells to induce long-term vascular normalization and tumor regression. *Proc Natl Acad Sci U S A* 2021;118:e2020057118.
24 Munn LL, Jain RK. Vascular regulation of antitumor immunity. *Science* 2019;365:544–5.
25 Gullino PM, Grantham FH. The vascular space of growing tumors. *Cancer Res* 1964;24:1727–32.
26 Hilmas DE, Gillette EL. Morphometric analyses of the microvasculature of tumors during growth and after x-irradiation. *Cancer* 1974;33:103–10.
27 Jain RK. Determinants of tumor blood flow: a review. *Cancer Res* 1988;48:2641–58.
28 Joseph RW, Elassaiss-Schaap J, Kefford R, *et al*. Baseline tumor size is an independent prognostic factor for overall survival in patients with melanoma treated with pembrolizumab. *Clin Cancer Res* 2018;24:4960–7.
29 Dall'Olio FG, Marabelle A, Caramella C, *et al*. Tumour burden and efficacy of immune-checkpoint inhibitors. *Nat Rev Clin Oncol* 2022;19:75–90.
30 Soon YY, Tan TH, Lee CK, *et al*. Machine learning predicted fast progression after initiation of immunecheckpoint inhibitors in advanced non-small cell lung cancer. *BMJ Oncology* 2024;3:e000227.
31 Hatfield SM, Sitkovsky MV. Antihypoxic oxygenation agents with respiratory hyperoxia to improve cancer immunotherapy. *J Clin Invest* 2020;130:5629–37.
32 Noman MZ, Desantis G, Janji B, *et al*. PD-L1 is a novel direct target of HIF-1α, and its blockade under hypoxia enhanced MDSC-mediated T cell activation. *J Exp Med* 2014;211:781–90.
33 Kalbasi A, Ribas A. Tumour-intrinsic resistance to immune checkpoint blockade. *Nat Rev Immunol* 2020;20:25–39.
34 Huang Y, Kim BYS, Chan CK, *et al*. Improving immune-vascular crosstalk for cancer immunotherapy. *Nat Rev Immunol* 2018;18:195–203.
35 Sun R, Limkin EJ, Vakalopoulou M, *et al*. A radiomics approach to assess tumour-infiltrating CD8 cells and response to anti-PD-1 or anti-PD-L1 immunotherapy: an imaging biomarker, retrospective multicohort study. *Lancet Oncol* 2018;19:1180–91.
36 Alilou M, Khorrami M, Prasanna P, *et al*. A tumor vasculature-based imaging biomarker for predicting response and survival in patients with lung cancer treated with checkpoint inhibitors. *Sci Adv* 2022;8:eabq4609.